DESIGN AND IMPLEMENTATION OF A TRANSCEIVER AND A MICROSTRIP CORPORATE FEED FOR SOLID STATE X-BAND RADAR

By

Mauricio Sánchez Barbetty

A thesis submitted in partial fulfillment of the requirements for the degree of

MASTER OF SCIENCES
in
ELECTRICAL ENGINEERING

UNIVERSITY OF PUERTO RICO
MAYAGÜEZ CAMPUS

2005

Approved by:

Sandra L. Cruz-Pol, PhD Member, Graduate Committee	Date
Rafael Rodriguez Solís, PhD Member, Graduate Committee	Date
José Colom Ustáriz, PhD President, Graduate Committee	Date
Walter Diaz, PhD Representative of Graduate Studies	Date
Isidoro Couvertier, PhD Chairperson of the Department	Date

ABSTRACT

The design of a corporate feed for an X band frequency scanned microstrip antenna array and a surface mount transceiver are presented. The power distribution generated by the corporate feed network is based on a Taylor distribution to obtain an antenna sidelobe level below 20dB in the azimuth direction. The design of a surface mount transceiver is also presented as the first step in the evolution of the frequency scan antenna into an active antenna with electronic beam steering in the azimuth plane. This work is part of the development of a solid state radar for weather applications, constructed in collaboration with the University of Massachusetts at Amherst and sponsored by the NSF Collaborative Adaptive Sensing of the Atmosphere Engineering Research Center.

To my family . . .

Acknowledgements

During the development of my graduate studies in the University of Puerto Rico several persons and institutions collaborated directly and indirectly with my research. Without their support it would be impossible for me to finish my work. That is why I wish to dedicate this section to recognize their support.

I want to start expressing a sincere acknowledgement to my advisor, Dr. José Colom Ustáriz because he gave me the opportunity to research under his guidance and supervision. From him, I received motivation, encouragement and support during all my studies. I also want to thank Dr. Rafael Rodríguez Solís who taught me most of the things that I know about microwave circuits and antennas. I also want to express my gratitude to Dr. Sandra Cruz Pol for all the instructions that she gave me to make oral presentations, writing papers and sharing my ideas to the public in a more effective way.

I also want to thank Víctor Marrero and Jose Maeso, graduate students of UPRM, for being sources of extremely useful information in many fields besides the engineering related ones. To Eric Knapp from UMASS for the guidance in the development of the transceiver. To Jorge Salazar from UMASS who designed the antenna columns. To Rosa Arroyo and Claribel Lorenzo, administrative staff from UPRM, for all the help in the purchasing orders, travels arrangements and money related things during my two years of residence in Puerto Rico.

This work is supported primarily by the Engineering Research Centers Program of the National Science Foundation under NSF award number 0313747. Any opinions, findings, conclusions, or recommendations expressed in this material are those of the authors and do not necessarily reflect those of the National Science Foundation.

At last, but most importantly I would like to thank my family, for their unconditional support, inspiration and love.

Table of Contents

Table List

Tables **Page**

Figure List

Figures **Page**

1 INTRODUCTION

1.1 Motivation

The work presented here is developed as part of the Collaborative Adaptive Sensing of the Atmosphere (CASA) and sponsored by the National Science Foundation (NSF) Engineering Research Center (ERC). CASA's vision is to revolutionize our ability to observe the lower troposphere through Distributed Collaborative Adaptive Sensing (DCAS), vastly improving our ability to detect, understand, and predict severe storms, floods, and other atmospheric and airborne hazards [*CASA Strategic Plan*, 2003].

National Weather Service (NWS) today's atmospheric observation approaches rely mostly on NEXRAD (next generation weather radar), which is a 50-year old network composed of 138 long-range (more than 200 km) Doppler radars in the United States and one in Puerto Rico. The radar sensors work independently; have low sensitivity and its long-range limits the resolution. Also, the earth's curvature prevents the lower boundary layer from being observed at far distances from the radar, missing important information [*Skolnik*, 2001].

The objective of DCAS is to create a low-cost and low-power radar network designed to overcome the fundamental limitations of current approaches to sensing and predicting atmospheric hazards. Distributed refers to the use of large numbers of solid-state radars, spaced appropriately, to overcome blockage due to the Earth's curvature, resolution degradation caused by beam spreading, and large temporal sampling intervals resulting from today's use of mechanically scanned antennas. Collaboratively refers to the possibility of these radars to operate via coordinated targeting of multiple radar beams, based on atmospheric and hydrologic analysis tools (detection, tracking and predicting algorithms). Adaptive refers to the ability of these radars and the associated computing and communications infrastructure to rapidly reconfigure in response to changing conditions in a manner that optimizes response to competing end user demands.

The first generation of CASA radars used for the first test bed located in Oklahoma are expensive magnetron radars mounted on mechanical positioners. These radars will operate at X band with a center frequency of approximately 9.483GHz which is the center frequency of the magnetron oscillator. Some of the generations proposed in order to make a transition from the first generation of magnetron CASA radars to solid-state radars are shown in Figure 1.1. The main characteristic of this evolution is an antenna capable of steering its beam electronically allowing the radar to rapidly adapt to the needs of the system and the sensing conditions. The first step in the evolution of the antenna (generation III) is a microstrip array capable of steering its beam in elevation with frequency changes at the input of each column of the array, the azimuth scanning is still mechanical for this generation. Prototypes of this antenna are being developed at the University of Puerto Rico at Mayagüez and the University of Massachusetts at Amherst. An RF power distribution network called the Corporate Feed feeds the array of columns. The function of the corporate feed is to distribute the RF signal with the proper amplitudes and the same phase to each column in order to achieve the desired radiation pattern in the azimuth direction. The Corporate Feed also needs to have the bandwidth required by the antenna to properly perform the frequency scanning in the elevation direction.

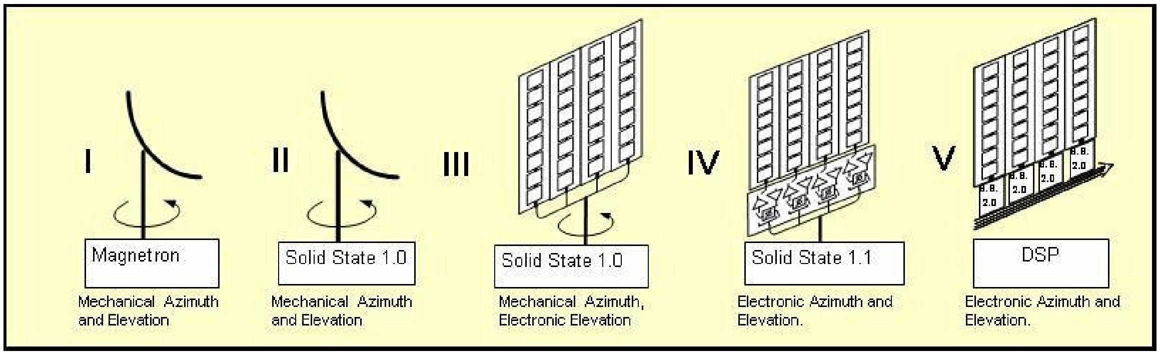

Figure 1.1 CASA Radar Generations

For the fourth generation a transceiver and a phase shifter are going to be added to reduce the power needed from the principal RF source and to control the azimuth scanning electronically. The two components presented here, as parts of the current research, are the corporate feed and the transceiver for the generation 3 and generation 4 radars respectively.

1.2 Literature Review

Microstrip arrays antennas have been, during the last four decades, a frequent alternative for wireless systems, satellite communications and radars. These types of antennas have advantages such as low weight, thin profile, easy fabrication and low cost. Additionally, the use of phased array antennas allows advantages that other type of antennas do not have, like beam steering and multiple beams, eliminating mechanical scanning which usually consumes more power and due to its inertia is much slower than electronic scanning.

There are different methods to feed a microstrip array, among them is feeding in series, feeding in parallel using a corporate feed, spatial combiners, reflect arrays and lens antennas among others. Usually the first two methods are the simplest of all since they can be on the same layer of the array allowing optimization of the weight, thickness and costs of the antenna, whereas the others require more complex three-dimensional structures. However, feed resistive losses and radiation losses have to be taken into consideration when feed is coplanar to the array since they limit the gain and the radiation pattern [*Hall*, 1988].

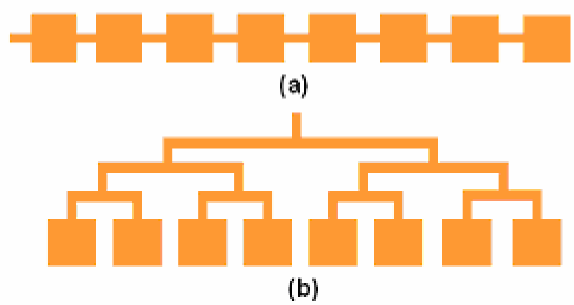

Figure 1.2 Microstrip Patch Arrays, (a) Series Feed (b) Parallel Feed

The series feed and the parallel feed are different in many aspects, first the parallel feed provides a larger bandwidth, generally 10% of the operation frequency, while the series feed provides bandwidths from 1 to 3 percent [*Huang*, 2003]. The main disadvantage of the parallel feed is that it suffers from more ohmic losses since the structures used for feeding in parallel occupy more space. The losses by radiation are also greater due to the amount of discontinuities needed in the parallel configuration. Combinations of both types of feeding are usually used to achieve an acceptable tradeoff between bandwidth, radiation losses, Ohmic losses and space; the antenna in figure 1.3 is a sketch of the proposed generation III of CASA radars.

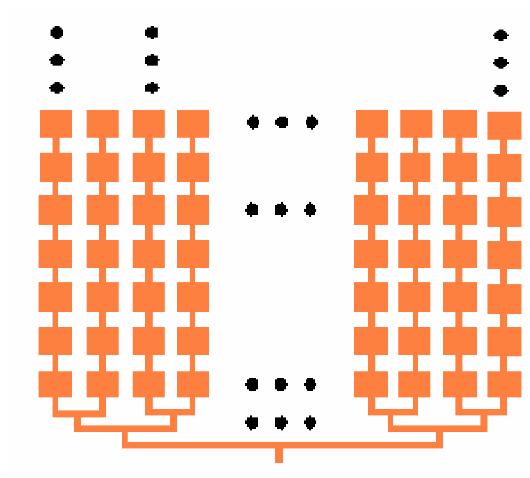

Figure 1.3 Microstrip Patch Antenna for Generation III

Similar Prototypes of antennas at X band with fewer elements can be found in [*Horng, et al.,* 1993] and [*Wang, C.F., et al.,* 1998]. In [*Levyne, et al.*, 1989] the effects of increasing the numbers of elements in parallel feeds have been studied. The proposed antenna is a composite of 64 columns each one composed of 64 patches or elements. The series feed of each column must allow beam scanning in elevation in the specified bandwidth; the design of this column is taken place at this moment at the University of Massachusetts at Amherst. The design of the parallel feed or corporate feed as it is usually called must provide the power distribution necessary to maintain the sidelobe level in azimuth below the specifications through the whole bandwidth.

In order to make the corporate feed, the different structures used as power dividers in microstrip circuits have been evaluated, the more commonly used are the T-junction, the Wilkinson power divider, the Quadrature (90°) hybrid also known as Branch line coupler, the coupled line coupler and the 180° hybrid or Rat Race [*Pozar,* 2004]. The most commonly used is the T-junction, but antenna arrays have been reported using quadrature hybrids and 180° hybrids in [Wang, J, et al, 19899], [*Huang, J.,* 1991], [*Sawichi, A., et al,* 1998] and others. The main advantage of the T-junction is simplicity in the design; the disadvantage is that it does not provide isolation between output terminals. The Wilkinson power divider overcomes the isolation between outputs problem by adding a resistive element and has the advantage that its input and output power are not consumed in the isolating resistor, but the losses become significant when the incoming signals from the output ports are out of phase. The quadrature hybrid and the 180° hybrid also provide good isolation between output ports and good combination of incoming signal when they are in phase but they usually occupy more space. In practice, if one of the output ports is mismatched, the reflected power will be absorbed in the matched load, maintaining the input matched.

It can be demonstrated that disregarding the number of elements in an array, when the power distribution is uniform, the best sidelobe level that can be obtained is 13.46dB [*Balanis,* 1996]. This is why the type of power splitter to be chosen must allow a tapering in amplitude so that sidelobe levels can be increased to the specifications level (20dB). Different types of power distributions are used to reduce the sidelobe level of an array; but within the most used are, the binomial distribution, the Dolph-Chebyshev, triangular distribution and the Taylor distribution. The corporate feed must provide a power distribution that allows beam steering avoiding grating lobes.

After designing the corporate feed, a transceiver for each column of the array will be designed, therefore reducing the power consumption from the main oscillator for transmission and at the same time, allowing the use of phase shifters for electronic beam steering in azimuth as shown in Figure 1.4. With this architecture, the radar would have 4 panels, each one with 64 columns; each panel should be able of achieving 90° of the 360° required for the azimuth scanning. The antenna array also requires an 800MHz bandwidth to obtain a 15° scan in elevation.

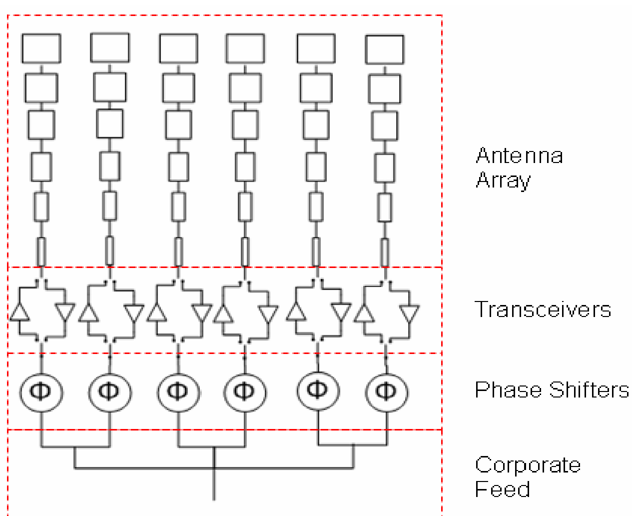

Figure 1.4 Generation IV Architecture

1.3 Summary of Following Chapters

We will first develop the necessary background theory and motivation from Chapter 1. Chapter 2 explains the procedures for the corporate feed; including design, simulation, and measurement of the performance obtained in some prototypes built at UPRM facilities. The third chapter presents the design of the transceiver and some implications of using this transceiver in the antenna of the generation IV radars. Chapter four concludes this thesis, presenting the conclusions and suggesting improvements as a part of the findings of this work.

2 CORPORATE FEED

2.1 S parameters and efficiency

The losses associated with the corporate feed are caused by factors such as: radiation losses, surface wave excitation and ohmic and dielectric losses. These losses represent a decrease in the output power of the corporate feed for a given input; which implies a lower efficiency of the antenna and the degradation of the radiation pattern. To analyze the efficiency of the corporate feed the S-parameters [*Pozar,* 2004] are going to be used as a measure of the total losses.

Consider a corporate feed having one input port and 64 output ports as shown below.

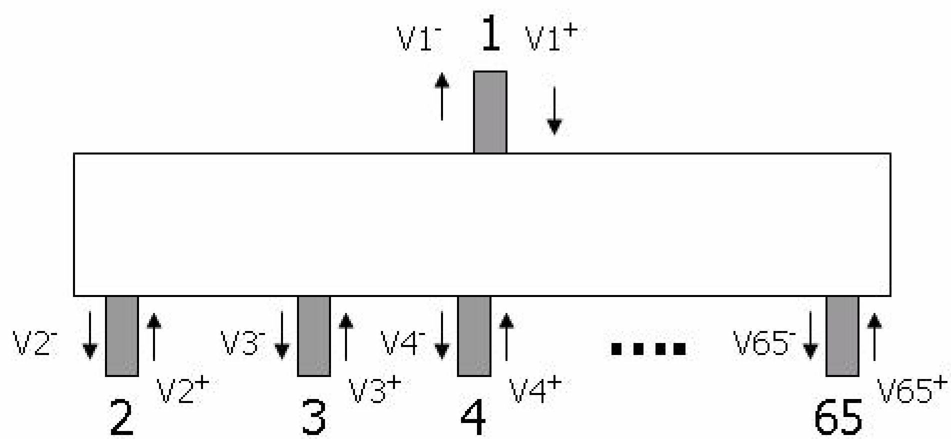

Figure 2.1 A 64 Element Corporate Feed

Assuming that the input and outputs are matched, for a given incident wave at port 1, the reflected voltage V_1^- becomes zero and the output voltages are the out coming waves

V_j^- for j =2 to 65, where j is the number of the port. The power delivered to the input of the divider is

$$P_{IN} = \frac{\left|V1^{+}\right|^{2}}{2Z_{0}} \qquad \textbf{2.1}$$

While the output powers are

$$P_{j,OUT} = \frac{\left|V_{j}^{-}\right|^{2}}{2Z0} \; j = 2,3,\ldots,65 \qquad \textbf{2.2}$$

The total output power is the sum of the power of all output ports and is given by

$$P_{OUT} = \sum_{j=2}^{65} P_{j,OUT} = \frac{\left|V_{2}^{-}\right|^{2}}{2Z_{0}} + \frac{\left|V_{3}^{-}\right|^{2}}{2Z_{0}} + \frac{\left|V_{4}^{-}\right|^{2}}{2Z_{0}} + \ldots + \frac{\left|V_{65}^{-}\right|^{2}}{2Z_{0}} \qquad \textbf{2.3}$$

Consider the efficiency defined as the ratio between the output and input powers as

$$\eta = \frac{P_{OUT}}{P_{IN}} = \frac{\sum_{j=2}^{65} P_{j,OUT}}{P_{IN}} = \frac{\dfrac{\left|V_{2}^{-}\right|^{2}}{2Z_{0}} + \dfrac{\left|V_{3}^{-}\right|^{2}}{2Z_{0}} + \dfrac{\left|V_{4}^{-}\right|^{2}}{2Z_{0}} + \ldots + \dfrac{\left|V_{65}^{-}\right|^{2}}{2Z_{0}}}{\dfrac{\left|V_{1}^{+}\right|^{2}}{2Z_{0}}} \qquad \textbf{2.4}$$

Equation 2.4 can be written in terms of the S-parameters as

$$\eta = \frac{\left|V_{2}^{-}\right|^{2}}{\left|V_{1}^{+}\right|^{2}} + \frac{\left|V_{3}^{-}\right|^{2}}{\left|V_{1}^{+}\right|^{2}} + \ldots + \frac{\left|V_{65}^{-}\right|^{2}}{\left|V_{1}^{+}\right|^{2}} = \left|S_{2,1}\right|^{2} + \left|S_{3,1}\right|^{2} + \ldots. + \left|S_{65,1}\right|^{2} \qquad \textbf{2.5}$$

The above equation will be used to calculate the total losses in the corporate feed and to compare the different types of power dividers. From this point of view, to improve the performance of a certain corporate feed it is necessary to minimize radiation, matching, ohmic and dielectric losses. Radiation losses in microstrip circuits are driven principally by the discontinuities of the structure, which are present mostly in corners and splitters. Ohmic and dielectric losses are associated to the dimensions and type of substrate chosen.

2.2 Power Divider

As a part of a preliminary analysis two types of well known power dividers mentioned in section 1.2 were analyzed to determine the more suitable for the corporate feed structure. These two power dividers are the Rat Race and the T-junction as shown in Figure 2.2.

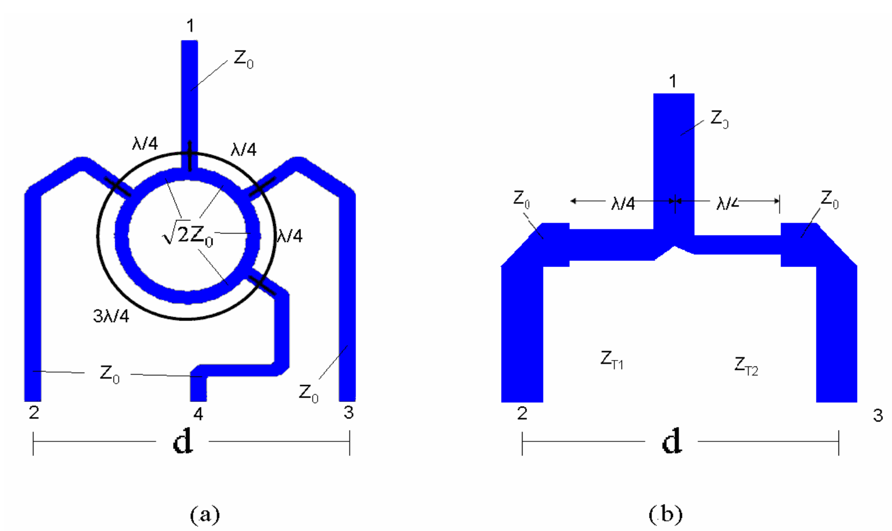

Figure 2.2 Power dividers (a) Rat race (b) T-junction

The separation distance d at the outputs of the power divider is going to be the separation of the antenna columns and is independent of the characteristics of the substrate. In order to have the same separation between output porst the Rat Race needs a substrate with higher permittivity to make the transmission lines shorter and thinner to comply with the space limitations. The main advantage of the Rat Race is the isolation between output ports but the disadvantage is that radiation, ohmic and dielectric losses are higher than the losses in a T-junction. Another disadvantage of the Rat Race is the need of a matching resistor in the isolated port (port 4) that generates more losses and makes the fabrication of the structure more complicated and more expensive.

On the other hand, the T-junction demonstrated to be a simple structure that requires a minimum of space allowing the use of a substrate of low permittivity and the possibility of having an unequal power division, which is necessary to implement amplitude tapering and improve the sidelobe level. The main disadvantage found in the T-junction is the poor isolation between outputs (near 6dB).

To obtain a quantitative measure of the efficiency of the two power dividers, two simulations of corporate feeds with uniform distributions were made in Advance Design System [*Agilent*, 2003], the first using 180° Hybrids (Rat Race) as power dividers and the second using T-junctions. The model used in this approach was the equivalent circuit model provided by the package, which reduces simulation time and is good for estimates but does no take in consideration coupling between lines and other geometrical effects. The S-parameters of the simulation were used to compute the efficiency according to equation 2.5 to compare the performance of the circuits and decide which power divider should be used. As shown in Figure 2.3(a), the estimated efficiency η of the corporate feed using 180° Hybrids is expected to be near 35% in the frequency range from 9 to 10

GHz. In the case of the T-junction the efficiency would be approximately 60% as shown in Figure 2.3(b), this difference was the main reason to choose the T-junction as the power divider to be used in the design of the power distribution network.

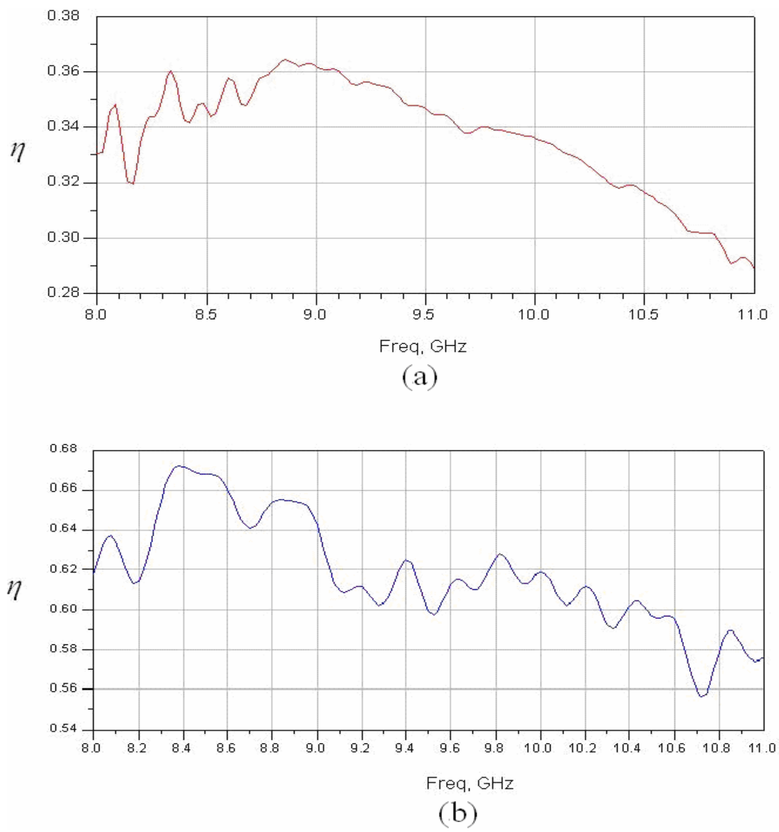

Figure 2.3 Estimated efficiency for a 64 outputs corporate feed. (a) Using 180° Hybrids (b) Using T-junctions.

2.3 Power Distribution

As mentioned before, the amplitude tapering must be made with the corporate feed to provide the necessary sidelobe level for the antenna. Using the pattern multiplication principle [*Balanis,* 1996], the power distribution provided by the corporate feed should produce the array factor that multiplied by the radiation pattern of one column will result in the radiation pattern of the whole antenna array. Considering the amplitudes of the outputs of the corporate feed as feeding coefficients of the array, the array factor can be written as

$$AF(\theta) = \left| \sum_{i=0}^{N-1} A_i e^{j\varphi_i} e^{jikd\cos(\theta)} \right|^2 \qquad \textbf{2.6}$$

Where A_i is the amplitude of the excitation coefficients, φ_i is the phase of each A_i, k is the propagation constant $k = 2\pi/\lambda$, d is the spacing between columns and N is the number of elements. For a broadside pattern as in generation III radars $\varphi_i = 0$ but for electronic scanning each φ_i is i times φ_o, where φ_o is calculated to be the position of the main lobe. In other words, the shape of the radiation pattern depends on the amplitude distribution of the A_i and the position on the main lobe depends on the phase shift between elements, φ_i.

Dolph [1946] introduced a method for calculating the amplitude coefficients Ai based on the Tschebyscheff recursion formula for polynomials (Equation 2.7).

$$T_m(z) = 2zT_{m-1}(z) - zT_{m-2}(z) \qquad \textbf{2.7}$$

This formula can be used to find one Tshebysheff polynomial if the polynomials of the previous two orders are known. The complete procedure to calculate the amplitudes and the array factor can be found in [*Balanis,* 1996]. This power distribution yields to a radiation pattern whose minor lobes are of equal intensity, with a main lobe of minimum beamwidth.

Taylor [1953] studied a power distribution that produces a pattern with inner minor lobes maintained at a constant level and the remaining ones decrease monotonically. In radar applications this is preferable because interfering or spurious signals would be further reduced when they try to enter through the decaying minor lobes. The source distribution is referred to as the Taylor (one-parameter) design and it given by:

$$I_n(z') = \begin{cases} J_0\left[j\pi B\sqrt{1-\left(\frac{2z'}{l}\right)^2}\right] & -l/2 \le z' \le l/2 \\ 0 & elsewhere \end{cases} \qquad \textbf{2.8}$$

Where J_o is the Bessel function of the first kind of order zero, l is the total length of the source and B is a constant to be determined from the specified sidelobe level. The disadvantage of designing an array with decaying minor lobes as compared to a design with equal minor lobe level (Dolph-Tschebysheff) is that it yields about 12 to 15% greater half-power beamwidth. However such a loss in beamwidth is a small penalty when extreme minor lobes decrease as $1/u$ where $u = \pi*(l/\lambda)*\cos(\theta)$ [*Balanis,* 1996]. In practice the Dolph-Tschebysheff distribution has the disadvantage of having grating lobes placed in θ=180°; for this reason, it was decided that the Taylor distribution is more suitable for the type of corporate feed needed.

2.4 64 Output Corporate Feed with Taylor Distribution

2.4.1 Design principles

To achieve the tapered power distribution of the corporate feed, the microstrip T-junctions were designed using the lossless transmission line model as show below.

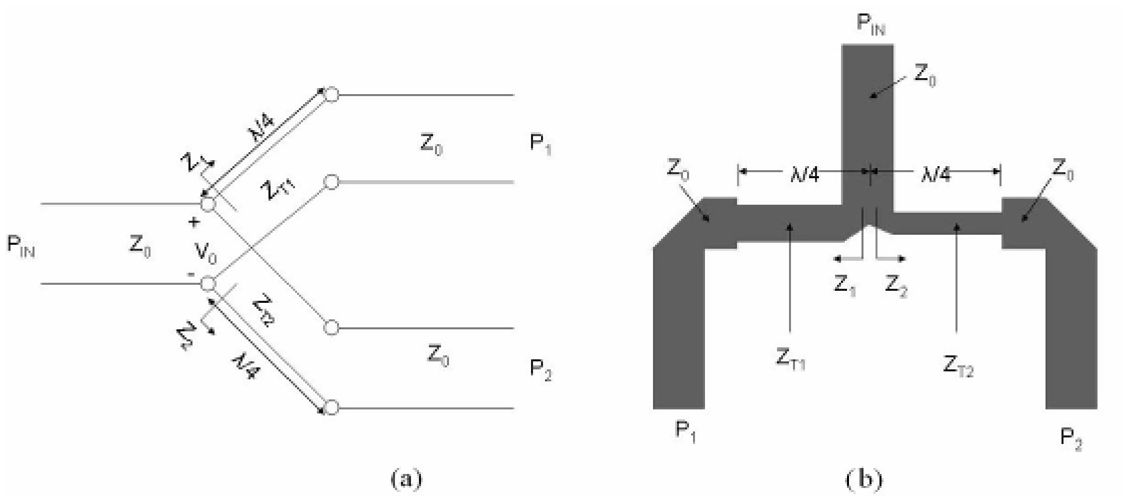

Figure 2.4 T-junction (a) Lossless transmission line model (b) Microstrip form.

If the voltage at the junction is V_o, as shown in Figure 2.4a, the input power to the matched divider is

$$P_{in} = \frac{1}{2}\frac{V_0^{\ 2}}{Z_0} \qquad \textbf{2.9}$$

While the output powers at each side of the junction are

$$P_1 = \frac{1}{2}\frac{V_0^{\ 2}}{Z_1} \quad , \quad P_2 = \frac{1}{2}\frac{V_0^{\ 2}}{Z_2} \qquad \textbf{2.10}$$

Since the lossless model is the one that is being used, the total output power $P_{out}=P_1+P_2=P_{in}$.

$$P_{OUT} = P_1 + P_2 = P_{IN} \qquad \textbf{2.11}$$

Therefore, for an unequal power distribution

$$P_1 = KP_{in}$$

$$P_2 = (1-K)P_{in} \quad 0 < K < 1 \qquad \textbf{2.12}$$

Combining equations 2.9 to 2.12 the impedances at each side of the matched junction can be obtained as

$$Z_1 = \frac{Z_0}{K}$$
$$Z_2 = \frac{Z_0}{(1-K)} \qquad \textbf{2.13}$$

Thus the total output impedance at the right side of the junction $Z_1 \| Z_2$ is equal to the input impedance and maintains the matched condition. The quarter-wave transformers Z_{T1} and Z_{T2} are calculated to match the transmission lines at the outputs of the divider with impedance Z_o to the desired impedance at the junction as

$$Z_{T1} = \sqrt{Z_0 Z_1}$$

$$Z_{T2} = \sqrt{Z_0 Z_2} \qquad \textbf{2.14}$$

In practice, the T-junction is not lossless and the output power $P_{out} = P_{in} - P_{loss}$ were P_{loss} is the sum of the dielectric, ohmic and radiation losses. The power ratio P_1/P_2 is very similar to the lossless case because, as shown in Figure 2.4, the microstrip form is almost symmetrical at both sides of the junction and the losses can be considered approximately equal from the input to each output of the divider.

To obtain the 20 dB sidelobe level Taylor coefficients for the 64 elements corporate feed the software PCAAD 3.0 [*Antenna Design Associates,* 1996] was used. The parameters to calculate the distribution are shown in Table 2-1.

Table 2-1 Parameters to obtain the Taylor distribution

Parameter	Value
Number of Elements	64
Spacing	1.7 cm
Sidelobe Level	20dB
N-Bar	2

The first 32 normalized amplitude and power coefficients are shown in Table 2-2, the next 32 elements are a mirror of the first 32 because the desired patter is symmetrical with respect to the center of the array.

Table 2-2 Normalized Amplitude and Power Coefficients for a Taylor Distribution

Port Number	Normalized Amplitude (Voltage)	Normalized Power
1	0.40384	0.16309
2	0.40672	0.16542
3	0.41245	0.17011
4	0.42098	0.17722
5	0.43221	0.18681
6	0.44606	0.19897
7	0.46238	0.21379
8	0.48101	0.23137
9	0.50178	0.25178
10	0.52448	0.27508
11	0.54890	0.30129
12	0.57480	0.33040
13	0.60194	0.36233
14	0.63004	0.39695
15	0.65885	0.43408
16	0.68809	0.47347
17	0.71749	0.51479
18	0.74678	0.55768
19	0.77571	0.60172
20	0.80402	0.64644
21	0.83144	0.69129
22	0.85769	0.73563
23	0.88245	0.77871
24	0.90540	0.81975
25	0.92627	0.85797
26	0.94482	0.89269
27	0.96089	0.92331
28	0.97433	0.94931
29	0.98501	0.97024
30	0.99285	0.98576
31	0.99783	0.99567
32	1.00000	1.00000

The impedances of the entire corporate feed can be calculated using equations 2.9 to 2.14 where P_1 and P_2 are Taylor coefficients and K is the relation between them. The input power to each T-junction can be assumed to be sum of P_1 and P_2. For example, in

Figure 2.5 the input power is $P_7 > P_5 + P_6$ because of the losses introduced by the lines, but to obtain the desired power ratio P_5/P_6 the assumption of $P_7 = P_5 + P_6$ is a valid approximation. To calculate Z_{T1} to Z_{T4} it can be said that $P_7 = P_1 + P_2 + P_3 + P_4$ as well.

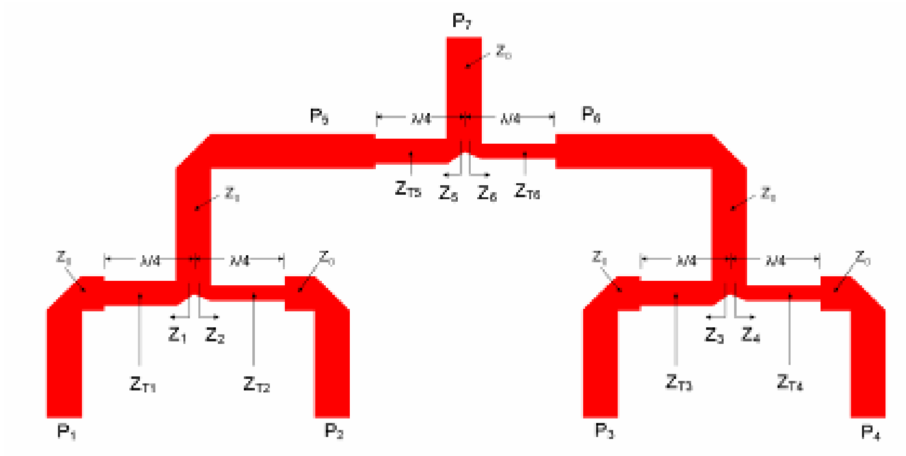

Figure 2.5 Example of tapered distribution

With the impedances calculated, the next step in our design was to choose a substrate and then calculate the physical dimensions using the software *Line Calc* [*Agilent*, 2003]. Table 2-3 summarizes the deductions relating to substrate choice [*Hall, et al,* 1988].

Table 2-3 Optimum substrate choice for array performance requirements

Requirement	Dielectric Constant	Substrate Thickness
1. Low feed radiation	High	Thin
2. Low surface waves	Low	Thin
3. Good tolerance control	Low	Thin
4. Low mutual coupling	Low	Thin
5. Low array losses	High	Thin
6. Wide Bandwidth	Low	Thick

Where, thin substrates are those whose thickness is lower than 30mil (0.762mm); for thick substrates the thickness is above 50mil (1.27mm). It can be seen in Table 2-3 that the efficiency increases by the use of thin substrates but at the expense of antenna element bandwidth. Decrease in substrate thickness are accompanied by reduced pattern perturbation due to feed radiation but for practical considerations substrates of 20 mil of thickness or less are mechanically difficult to handle at UPRM facilities. The requirements for the dielectric constant are also contradictory, with low dielectric constant leading to wider bandwidths but in particular increased array losses. Considering these trade-offs the following substrate was chosen:

- Permittivity: ε_r=2.2.
- Thickness: H = 31 mil.
- Copper cladding: 1oz (35μm).

Since cost is also an important consideration at the time of choosing the material, quotations from different companies where obtained for the electrical characteristics of the substrate. It was found that some companies (*Rogers Corp.*) can provide a material with the desired specifications but *Taconic* has a material with the same specifications at a lower price, the reference for this substrate is TLY-5-0310-C1/C1.

The final layout of the 64 outputs corporate feed is shown in Figure 2.6, the simulation results and analysis are shown in the next section.

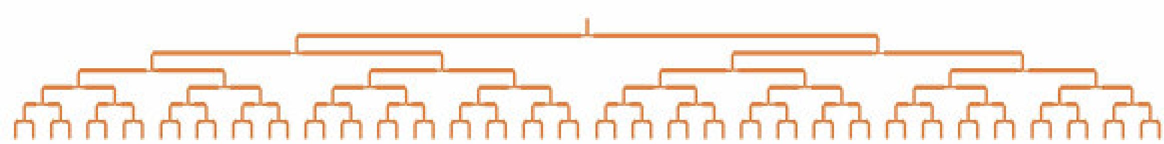

Figure 2.6 Layout for the 64 output corporate feed with a Taylor distribution

2.4.2 *Simulation Results*

The electromagnetic simulation of the Corporate Feed was made using Ansoft Designer [*Ansoft Corp*, 2002]. From this simulation the S parameters from 9 to 10GHz were obtained and analyzed using Matlab routines that calculated parameters such as the return loss, efficiency, array factor and some other parameters that will be presented in this section.

The return loss is shown in Figure 2.7, this parameters is also called the reflection coefficient at the input (S_{11}) and since it is below the -10dB in the range from 9 to 10GHz it can be concluded that the VSWR will be lower than 2 in the specified bandwidth.

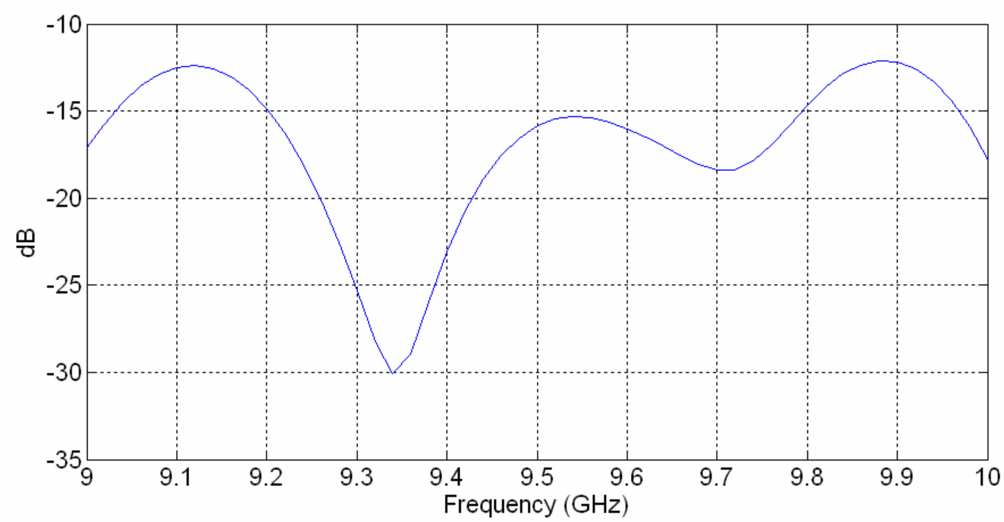

Figure 2.7 Return Losses for the 64 output corporate feed.

The 64 transmission coefficients S_{i1} with i=2 to 65 are shown in Figure 2.8, as the figure illustrates, the power distribution is maintained very similar throughout bandwidth. The comparison with the desired Taylor distribution is made in Figure 2.9 by normalizing the amplitudes at the center frequency and comparing them with the amplitude distribution provided by PCAAD.

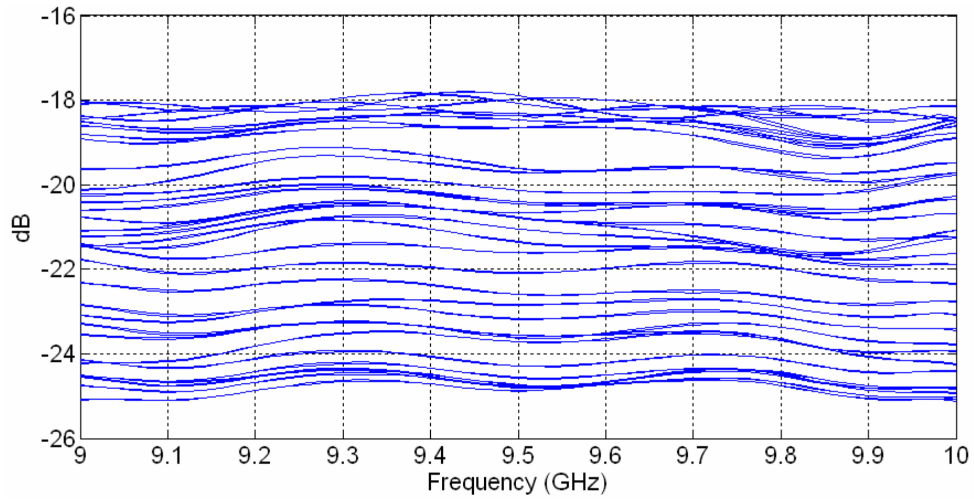

Figure 2.8 Transmission coefficients S_{i1} i=2,3,….,65

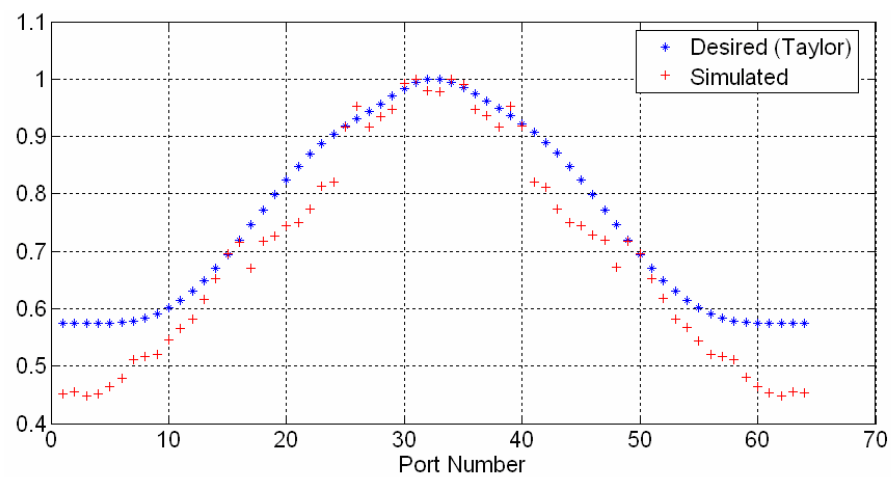

Figure 2.9 Normalized Amplitude Distribution at 9.5GHz

The radiation pattern of the antenna in the azimuth plane is the product of the array factor provided by the corporate feed by the radiation pattern of one antenna column plus the perturbation effects produced by the radiation losses of the corporate feed and the coupling effect between columns. The radiation losses can be isolated using special materials that will prevent the RF signal radiated from the corporate feed to reach far distances from the antenna. Since the radiation pattern and geometry of the column is not known the only quantity that can be calculated is the array factor, this was made using the transmission coefficients S_{i1} in equation 2.6. The comparison of the obtained array factor and the desired (provided by PCAAD) is made in Figure 2.10.

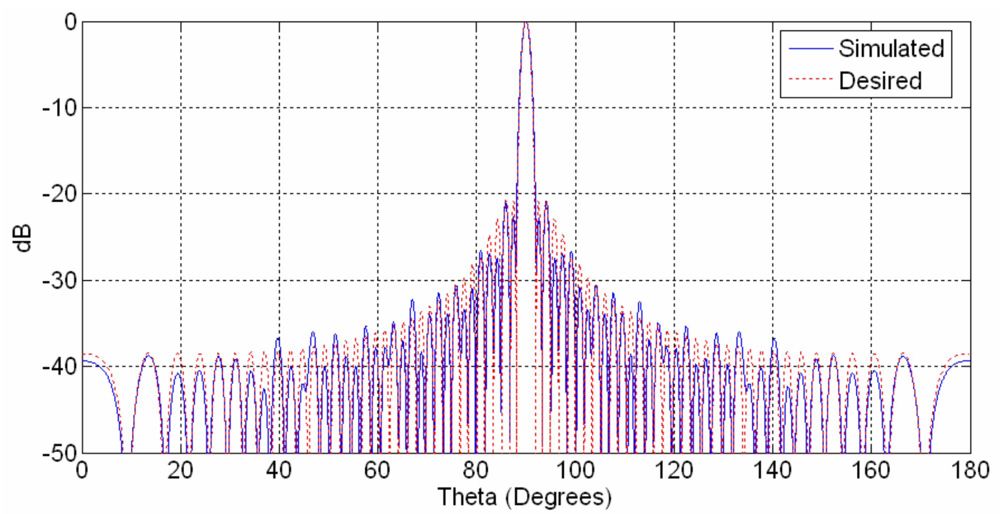

Figure 2.10 Array Factor at 9.5GHz

Figure 2.11 and Figure 2.12 show that the sidelobe level is above the 20dB and the beamwidth is below 2 degrees in the range from 9 to 10GHz. These results agree with the requirements for the system.

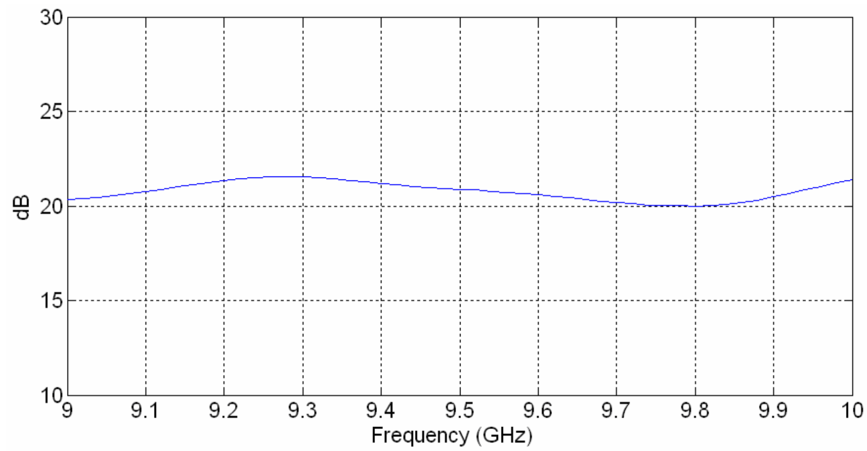

Figure 2.11 Sidelobe Level

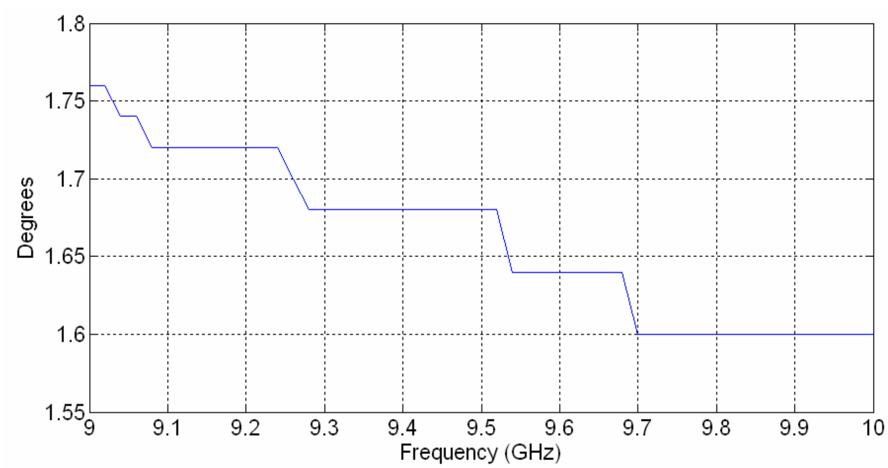

Figure 2.12 Beamwidth

The Efficiency (ratio between the input and output power) was calculated using the S-parameters in equation 2.5 and is shown in Figure 2.13. Given that this is a large power divider a relatively low efficiency is expected, still the efficiency is above 50% throughout all the bandwidth and is close to the efficiency expected using T-junctions as mentioned in section 2.2 (Figure 2.3).

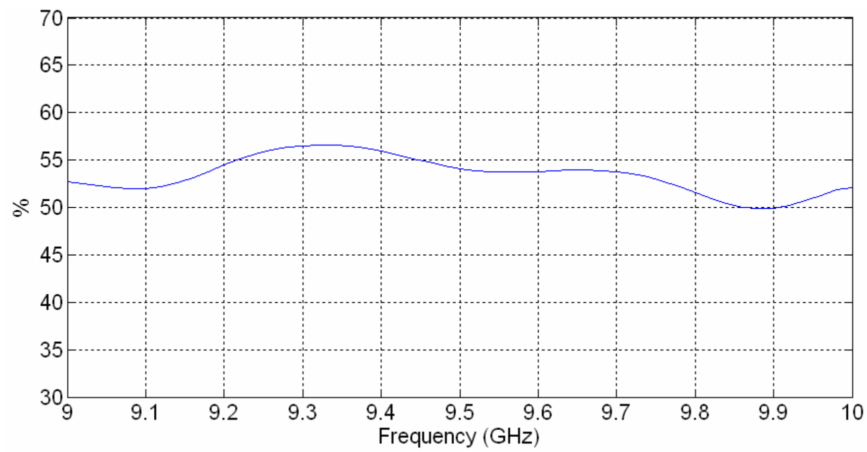

Figure 2.13 Efficiency

The next parameter to be analyzed is the coupling between outputs $S_{i,i+1}$, this is the amount of energy that reaches an output port when some energy enters from another output port next to it. The effects of a poor isolation between outputs is that any reflections from an antenna column will get into the next column multiplied by the isolation factor and will be radiated with a different phase and as a result the radiation pattern will be degraded. Figure 2.14 illustrates the coupling between outputs for the 64 outputs of the corporate feed. It can be observed that the worst case of coupling is near the 10GHz for approximately the half of the ports, which is usual for a T-junction given that the outputs are not designed to be isolated from each other.

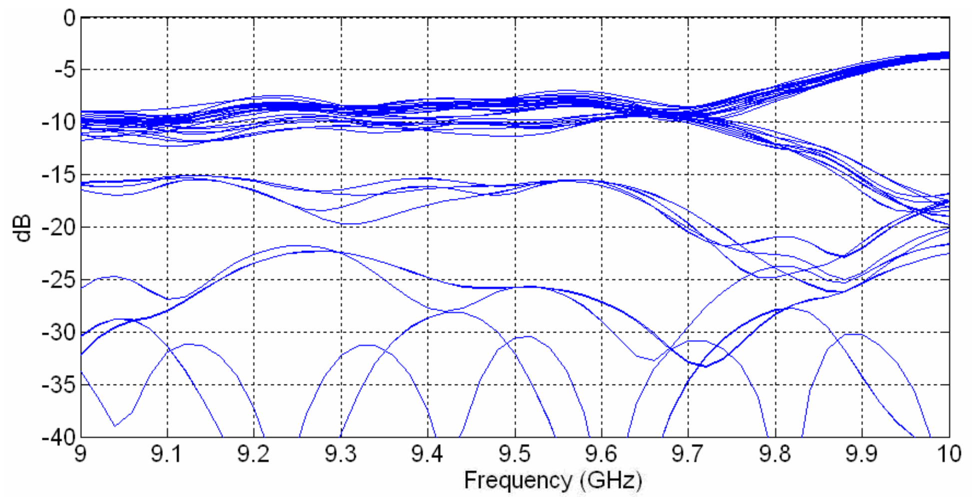

Figure 2.14 Coupling Between Outputs

2.5 Prototype Measurements

After the simulation of the corporate feed some prototypes were built using a milling machine available at the Applied Electromagnetic Laboratory of the University of Puerto Rico (See Figure 2.15). Although the precision of this fabrication process is not as good as the photo etching technique that will be used to build the final prototype of the antenna, some useful measurements of these prototypes were made that corroborate the simulation results.

The comparison between measurement and simulation results was made with a 16 outputs corporate feed with a Taylor distribution. The reason for using a smaller corporate feed is that the number of connectors is less, reducing the cost and time expended in the validation process. Figure 2.15 shows one prototype with 4 outputs, two with 16 outputs and one with 32 outputs. Connectors were soldered to the first 3 prototypes and 50Ω loads were used to match the ports while measuring the S-parameters with a two-port network analyzer.

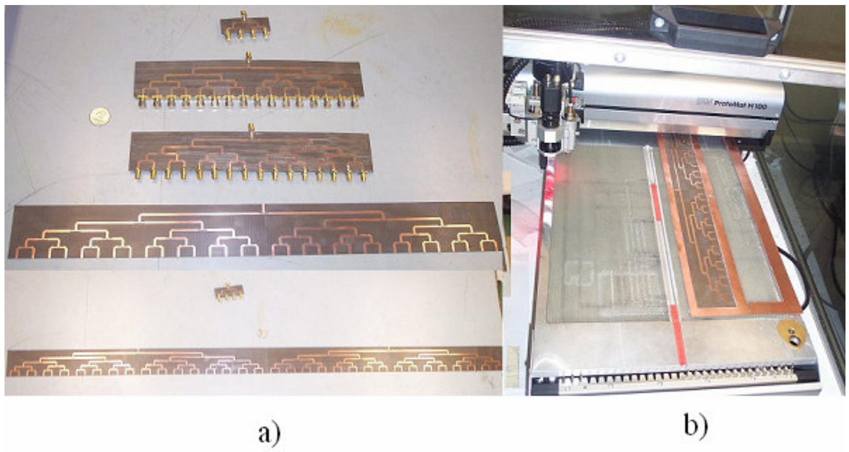

Figure 2.15 (a) Prototypes of corporate feeds (b) Milling machine at UPRM

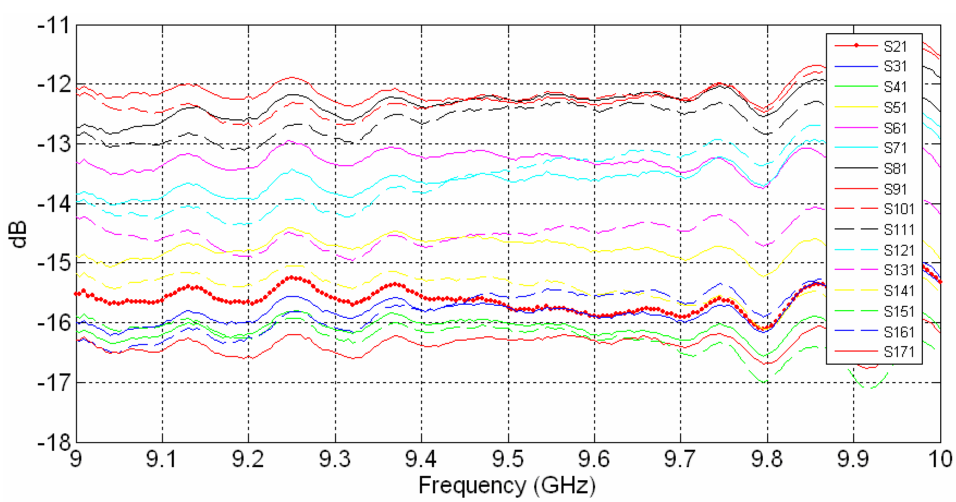

Figure 2.16 Measured Transmission coefficients of a 16 output corporate feed.

The 16 transmission coefficients S_{i1} with i=2 to 17 are shown in Figure 2.16, it is seen that the amplitude tapering is obtained through the entire bandwidth. The comparison with the desired Taylor distribution is made in Figure 2.17 by normalizing the amplitudes at the center frequency and comparing them with the amplitude distribution provided by PCAAD. Although some error can be seen, the effect of the difference between the desired and obtained power distributions is analyzed in the resulting array factor.

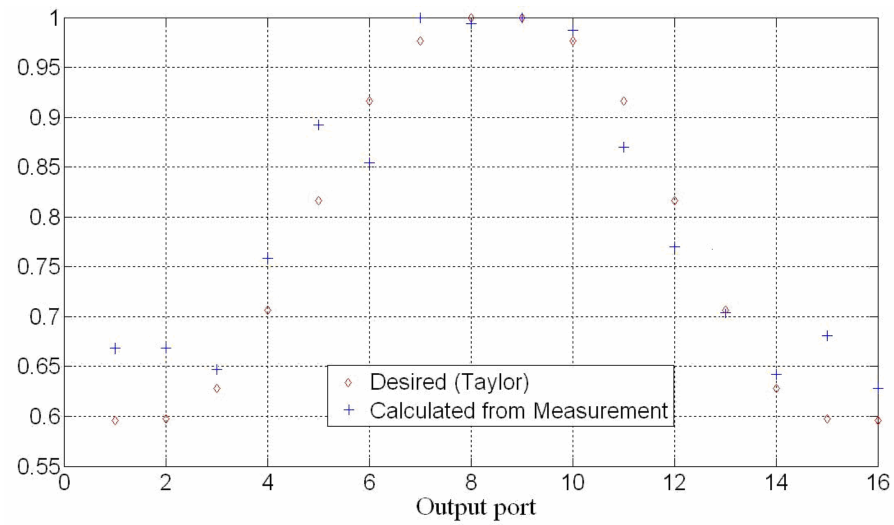

Figure 2.17 Normalized Amplitude Distribution at 9.5GHz

The array factor provided by the power distribution measured from the 16-output corporate feed is compared to the array factor of the desired Taylor distribution in Figure 2.18. The main difference found between the measured and desired results is the sidelobe level of the first two sidelobes. The cause for this is that the measured transmission coefficients include the reflections from all the ports connected to the low cost 50 ohms loads used to match the remaining ports. This effect is expected also in the 64-output corporate feed.

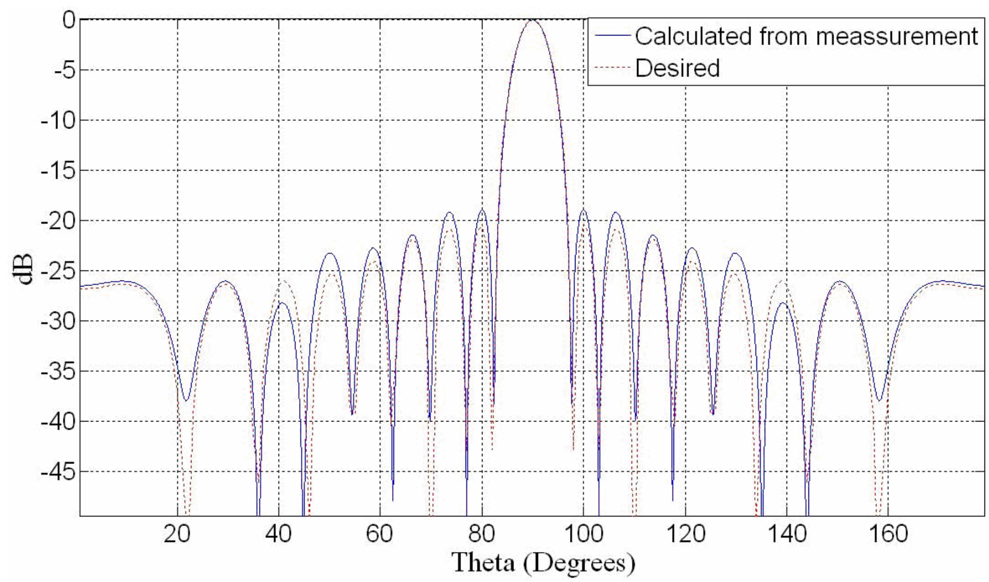

Figure 2.18 Array Factor at 9.5GHz

In general, measurement results agree very well with the simulations results. The agreement can be extended to the 64 output corporate feed in terms of power distribution and losses. The S parameters of the 64 output corporate feed will not be measured due to the size of the circuit and the number of connectors that would be needed. The 64 Outputs Corporate Feed with a Taylor distribution was etched with the antenna array during the summer of 2005.

3 SURFACE MOUNT TRANSCEIVER

3.1 Specifications and considerations

The purpose of the transceiver is to make a transition from generation III CASA radars to generation IV (See Figure 1.1). With a transceiver and a phase shifter at each column of the microstrip array, the mechanical scanning can be eliminated, this would reduce the power consumption and the power needed from the main oscillator, therefore a solid state low power oscillator can be used as the main source of the RF signal instead of the magnetron oscillator that is used in generation I CASA radars.

Some of the barriers that must be taken in consideration in this architecture are the space, costs and availability of components. Space is critical because the width of each transceiver should not exceed the separation (1.7cm) between columns; otherwise, it would have to be connected in a separate board perpendicular to the plane of the array and the cost will significantly increase. The cost should be minimized, because with this architecture the number of transceivers per panel is 64, each panel would handle 90 degrees of scanning in the azimuth direction, and as a consequence the radar would have 256 transceivers (four panels) to complete the 360 degrees of scanning. For example if the cost of a transceiver is one hundred dollars, the antenna system of the radar can exceed twenty five thousand dollars (256 x US$100.00), which is more than the cost expected for this radar. Another limitation was availability of surface mount components at X-band, which is limited at the present time. These constraints are due in part to the mounting and fabrication facilities at University of Puerto Rico in the field of surface mount technology. During the development of this project some companies released new surface mount components for X-band, for this reason it is expected that for future designs, the availability of components will improve.

Although the phase shifting circuit is not part of this research, the specifications of the phase shifter scheme directly affect the specifications of the transceiver. Figure 3.1 shows two schemes for the phase shifting; in the first one, the phase shift is made at an intermediate frequency IF and then the signal is up-converted to X-band. In the second scheme the phase shifting is performed at X-band after the mixing of the IF signal with the local oscillator. The main problem of the second method is that there are not many phase shifters available at X-band, and the few ones that were found during the development of this project are usually large, lossy and expensive. For this reason it was assumed that the first scheme will be used. In addition, the power levels handled by the transceiver at the input switch should match the power levels of a typical surface mount mixer.

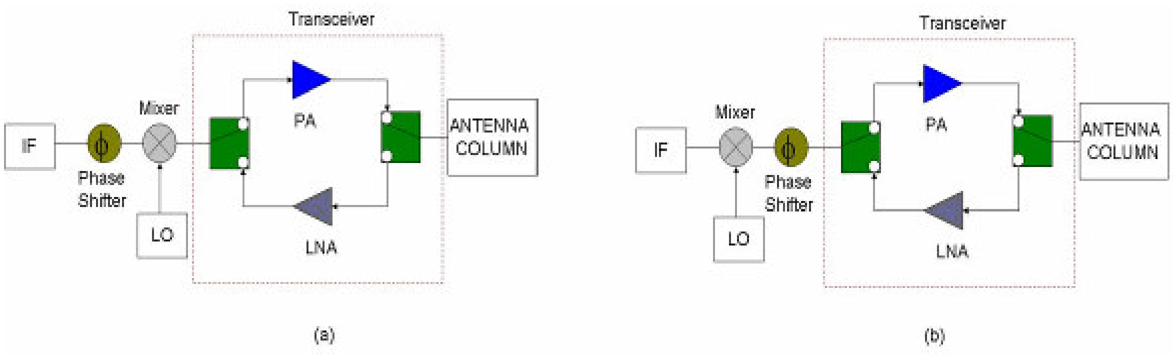

Figure 3.1 Phase shifter scheme (a) IF Phase shifter (b) RF Phase shifter

The radiated power for the entire microstrip array in the generation IV radar is expected to be between 30 and 100 Watts peak. This means that each transceiver needs to deliver from 0.5 to 1.5 Watts for each column of the array. An expression for the received power is illustrated in equation 3.1. In this version of the radar equation for meteorology [*Ulaby, F, et al*, 1981] the received power for a short pulse radar due to backscattering from volume-distributed incoherent scatterers is given by

$$P_r = \left[\frac{P_t G_0{}^2 \lambda_0{}^2 \beta_\theta \beta_\phi c \tau_p e^{-2\tau}}{32(4\pi R)^2} \right] \sigma_v \qquad \textbf{3.1}$$

Where P_t = Peak transmitted power
G_0 = antenna gain along the beam axis
λ_0 = wavelength
β_θ, β_ϕ = half power beamwidths in the azimuth and elevation plane of the antenna
c = velocity of light
τ_p = pulse length
τ = attenuation coefficient due to atmospheric gases, clouds and precipitation.
R = range to scattering volume
σ_v = volume backscatter coefficient

Almost all of these parameters are constant in the equation above, but the dependence on the range, the attenuation coefficient and the volume backscatter coefficient can make the received power to have variations of 80 decibels or more. Therefore, the most appropriate strategy is to increase the dynamic range of the receiver, in this way the weather measured by the radar can change from clear to intense rains maintaining the received power in a range above the noise floor and below the saturation level. It has to be taken into account also that, in reception, the signal power from all the transceivers are combined coherently, and the noise incoherently (assuming the individual amplifiers have uncorrelated noise), thereby the dynamic range is increased by 10log (N) dB, where N=64 is the number of elements for this case.

3.2 Surface mount transceiver prototype

Based on the specifications given in the previous section, the first prototype for the transceiver was made with available surface mount technology mainly from Hittite Microwave Corporation as shown in Figure 3.2.

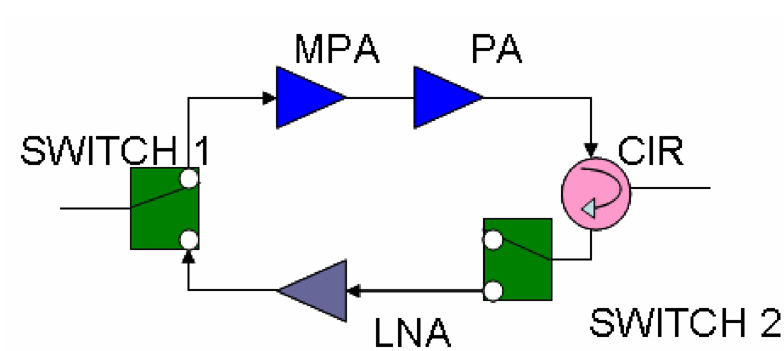

Figure 3.2 Surface Mount Transceiver

The reference designators are explained the table below.

Table 3-1 Reference Designators for Surface Mount transceiver

Ref. Des.	Part No.	Description	Company
SWITCH 1,2	HMC232LP4	GaAs MMIC SPDT Switch	Hittite
MPA	HMC441LP3	GaAs Phemt MMIC Medium Power Amplifier	Hittite
PA	HMC487LP5	Phemt 2 Watt Power Amplifier	Hittite
LNA	HMC516LP5	Phemt Low Noise Amplifier	Hittite
CIRCULATOR	C850115/DA	Microstrip Circulator	Track

At the input, the switch #1 HMC232LP4 controls the state of the circuit (transmit or receive). This switch has an insertion loss of 2dB at 10GHz and an isolation of 45dB. For transmission, the expected input power will be around 0 to 5dBm, the necessary gain to produce an output power of 30dBm (1Watt per column) is provided by the medium power amplifier (14dB) and the power amplifier (20dB). A circulator is necessary at the output because the switch has a 1dB compression point of 27dB and cannot handle the power of the PA; this circulator has an insertion loss of 0.5dB and an isolation of 20dB. The additional isolation provided by the switch 2 is to avoid more than 10dBm of input power to the LNA in transmission mode (RF maximum input power specified by the manufacturer). In reception, the low noise amplifier HMC516LC5 provides a noise figure of 2dB with a gain of 20dB. All the data sheets with the specification of these components can be found in Appendix 1. The substrate used for the board of the transceiver has a permittivity ε_r=9.7 and a thickness of 30 mil. The ADS schematic and Layout for this transceiver are shown in Figure 3.3 and Figure 3.4 respectively. The circuit has a width of 4.7cm and a length of 8.5cm.

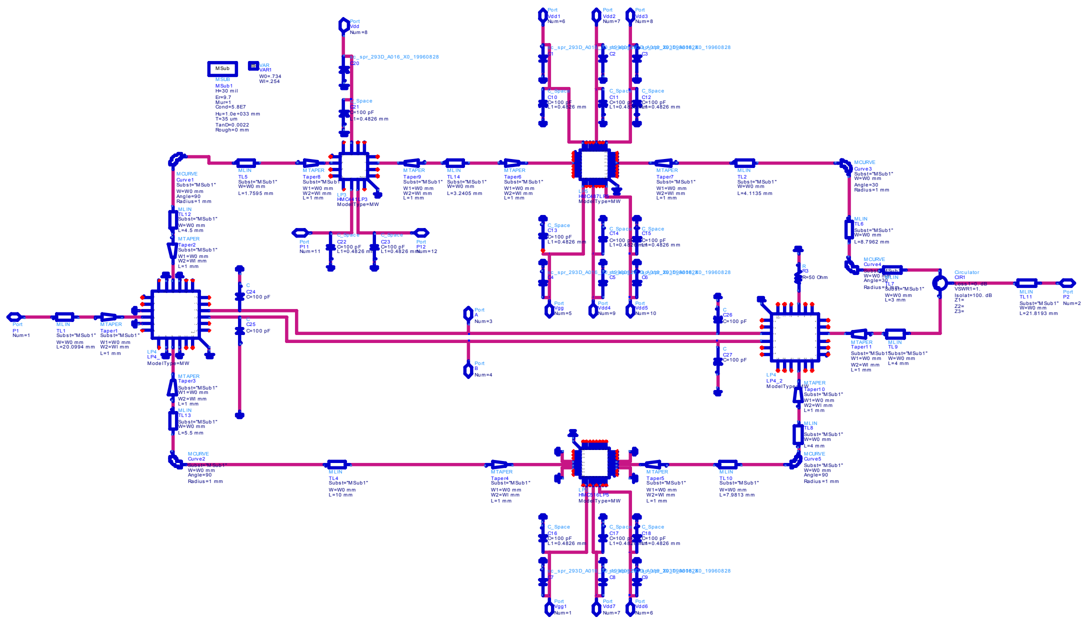

Figure 3.3 ADS Schematic for surface mount transceiver prototype

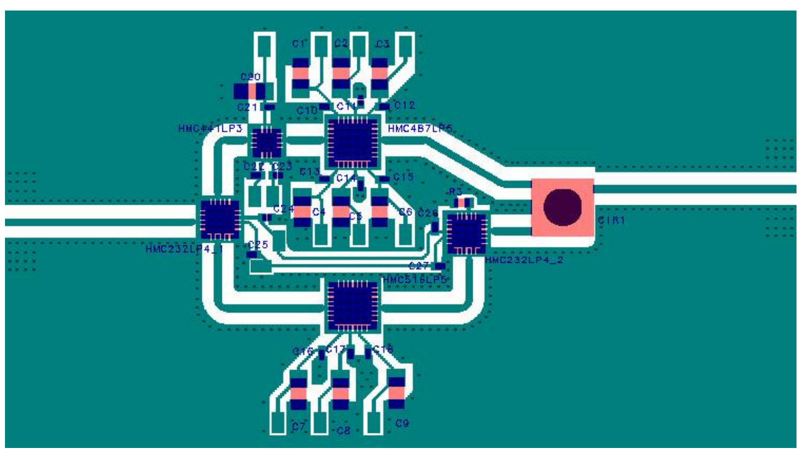

Figure 3.4 Layout of surface mount transceiver prototype

As the manufacturer of the switches and amplifiers does not provide a model for simulation, the measurements of the circuit need to be compared with the data sheets of the components. The circuit was built and tested for the first time obtaining results inferior to those expected due to the following reasons: The poor grounding made the LNA oscillate at frequencies near the 18GHz. The Switches did not provide the required isolation; instead of the expected 45dB it was 20dB. The insertion loss of the switches was 6dB instead of the 2dB expected. The gain of the PA stage was near the data sheet specification but the 1.3A@7V needed for the supply of the HMC487LP5 made the power dissipation of the circuit excessively high for the thermal configuration with a deficient heat sink.

3.3 Measurement of Evaluation Boards

Evaluation boards of the switch, PA and PNA were measured to recollect as much information as possible prior the design of a new transceiver. This section includes the measurement results of the evaluation boards for the HMC232LP4, HMC516LC5 and HMC487LP5 made with a two-port network analyzer.

The switch is a 3-port network, with port 1 being the input; port 2 the RF output connecting to the PA and port 3 connected to the LNA. When measuring the S-parameters of 2 ports the remaining one was connected to a 50 Ohm load similar to those used to measure the S-parameters of the corporate feed. Figure 3.5 show the S-parameter of the switch when the control connects port 1 to port 2 and isolates port 3. Figure 3.6 show the S-parameters when the control connects port 1 to port 3, isolating port 2.

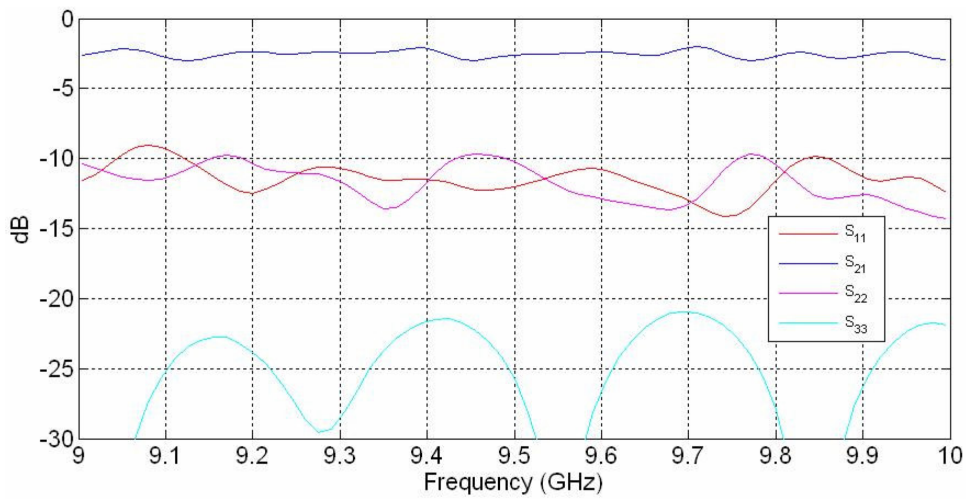

Figure 3.5 S parameters of the HMC232LP4, Port 1 to Port 2

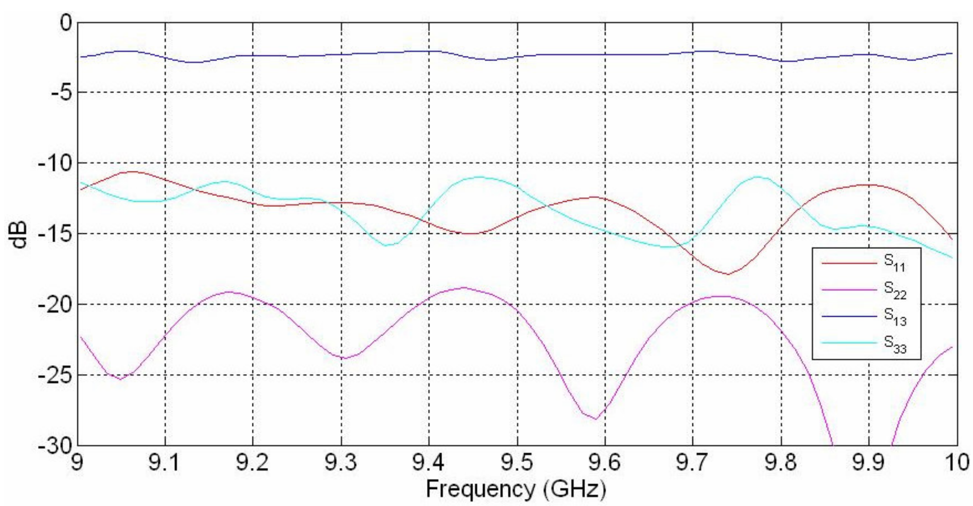

Figure 3.6 S parameters of the HMC232LP4, Port 1 to Port 3

As shown in the previous two figures, the insertion loss when two ports are connected is near 2.4dB in the range from 9 to 10GHz. The return loss is below 10dB for the connected ports and 20dB for the isolated port. The measured isolation was below 40dB.

Figure 3.7 shows the S parameters of evaluation board of the power amplifier. The measured gain agrees with the 20dB specified in the data sheet, but the power dissipation overheated the evaluation board causing the gain to decrease approximately 2dB after a few minutes of being turned on. This confirms that temperature and power dissipation are first priority issues if the same power amplifier is used in the final design.

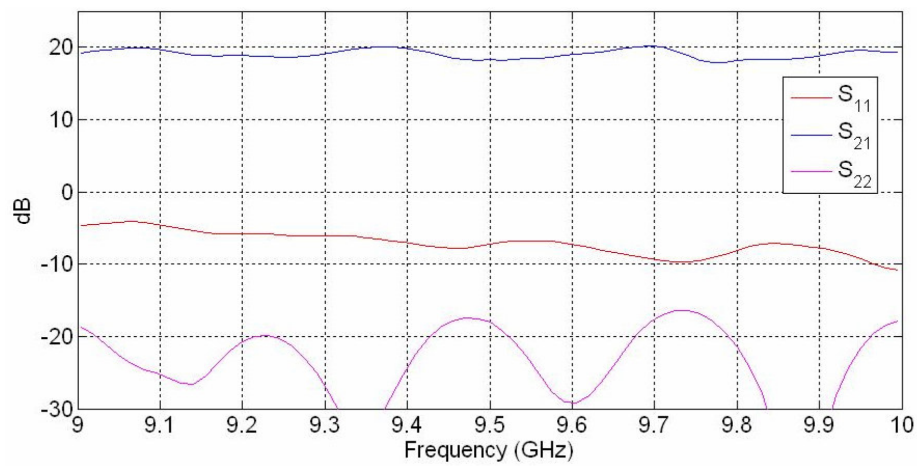

Figure 3.7 S-parameters of the HMC487LP5 evaluation board

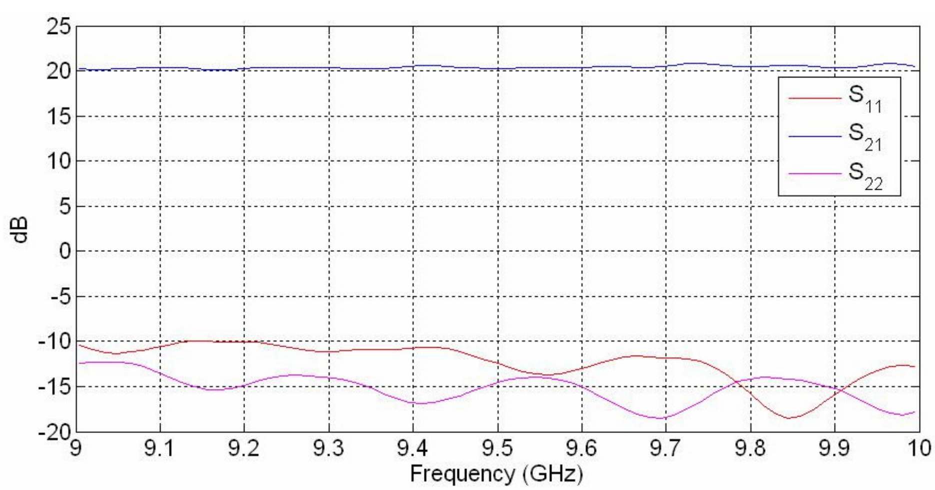

Figure 3.8 S-parameters of the HMC516LC5 evaluation board

The measurement of the LNA evaluation board also agreed with the specification of the data sheet as shown in Figure 3.8. The measured gain is 21dB and the return loss is below 10dB. The evaluation boards were also connected and measured in a transmitter stage and a receiver stage as shown on Figure 3.9. The closed loop was not made because only one evaluation board of the switch was available.

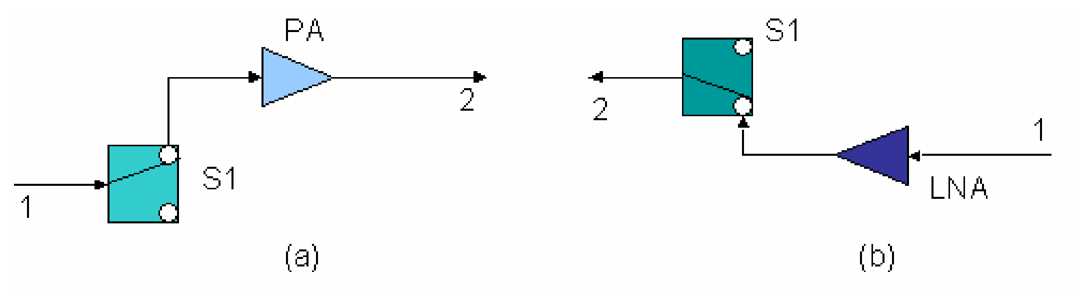

Figure 3.9 Diagram of connection (a) TX stage (b) RX stage

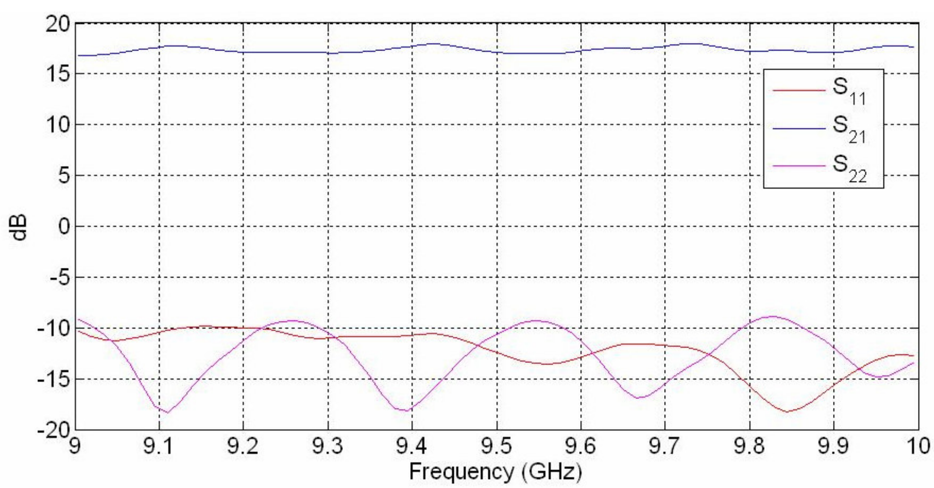

Figure 3.10 RX Stage S parameters

The S parameters of the RX stage are shown in Figure 3.10. For the TX stage the gain with the switch in the off state was also measured (S_{21OFF} in Figure 3.11), the value of –30dB is the addition of the isolation of –45dB of the switch with the gain of 18 dB of the power amplifier; a low value on this parameter is required to avoid oscillations when connecting the components in a closed loop.

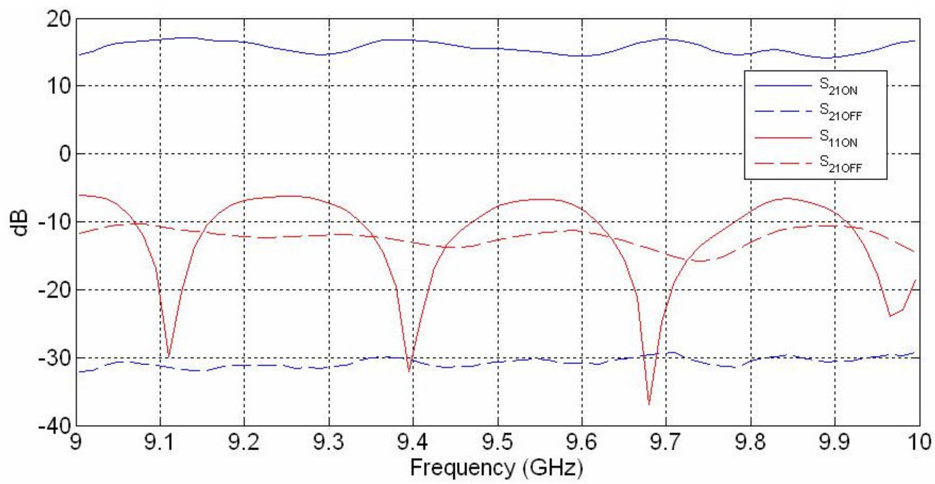

Figure 3.11 TX stage S parameters

In general the evaluation boards met the specifications of the data sheets. Based on the specifications of the material used and the type of transmission lines of the evaluation boards, the following recommendations are suggested to improve the performance of the transceiver circuit: The thickness of the substrate should be reduced to improve the grounding of the pads below the packages and to reduce the thermal resistance to the ground plane at the other side of the substrate. A heat sink needs to be attached to the ground plane to dissipate the heat produced by the power amplifier as shown in Figure 3.12. The pins that have not been used (NC) in all the packages should be connected to ground to reduce noise and improve stability in the amplifiers. Grounded coplanar wave guides instead of microstrip lines should be used because the MMICs inside the packages are designed for coplanar feed, avoiding a transition from microstrip to coplanar wave guide will reduce return losses and improve the matching between components.

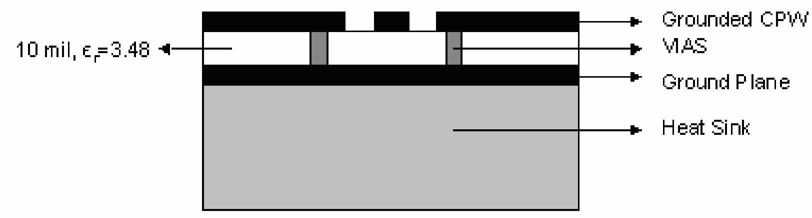

Figure 3.12 Side view of grounded coplanar wave-guide with heat sink

3.4 Improvements to the Surface mount transceiver

In addition to the suggested improvements mentioned in the previous two sections. An additional change in the proposed design is made based on the cost of the circulator. A Microstrip circulator [*Renaissance Electronics Corp*, 2005] or a Drop-in circulator [*TRAK Microwave Corporation*, 2005] is priced at approximately US$250; this means that for a panel of 64 transceivers, the circulators will cost US$16,000. In addition, the circulator requires a hole in the circuit, which increases the cost of each board. The penalty for eliminating the circulator is that the switch HMC232 has a 1dB compression point of 27dBm reducing the maximum output power to ~0.5W per transceiver (32 Watts for the entire array).

The ADS schematic and Layout for the improved transceiver are shown in Figure 3.13 and Figure 3.14, respectively. The material used for this design is the same as the evaluation boards of the HMC516LC5 and HMC487LP5, a Duroid RO4350 with 10mil of thickness and 1oz (35um) of Copper cladding [*Rogers Corp,* 2005].

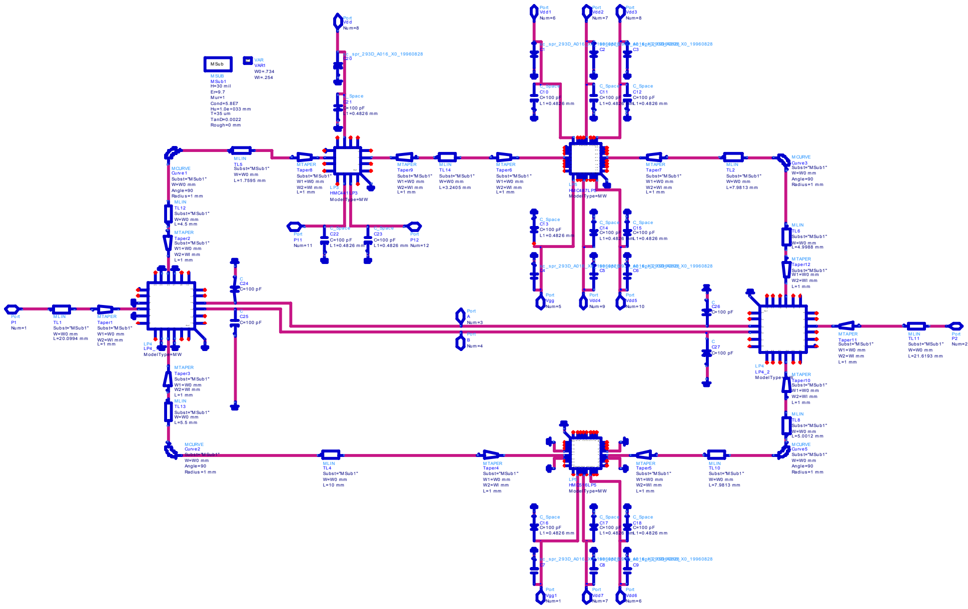

Figure 3.13 Schematic for the transceiver without circulator

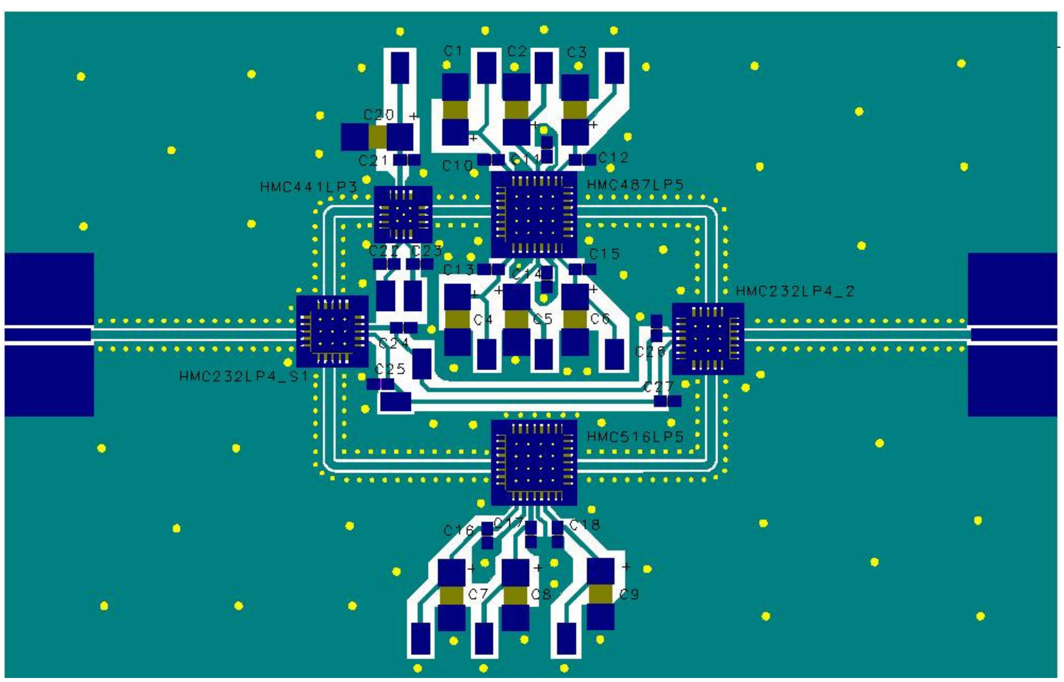

Figure 3.14 Transceiver layout without circulator using GCPW

The dimensions of this transceiver are 4.7cm x 7.4cm, which is almost 3 times the separation between antenna columns in the array. As mentioned in section 3.1, to connect the 64 transceivers it is necessary to put each one of them perpendicular to the array unless the size is reduced to less than 1.7cm in width. Another limitation of this circuit is the low efficiency and the need of a refrigerating system due to the power consumption of the PA for biasing.

The performance of the circuit in an array would also be determined by the phase shifting circuit used and the IF combining circuit which at the moment are not completely defined. For these reasons and because of the time constrains of this project, the fabrication of the circuit will be postponed until all the limitations have been solved or until a better solution is proposed. In the section of conclusions and future work some of the alternative solutions are discussed.

4 CONCLUSIONS AND FUTURE WORK

A microstrip power divider with 64 outputs and a Taylor distribution to obtain a sidelobe level below the 20dB and a 3dB beamwidth of 2 degrees was presented. The analysis of the performance was made using the S parameters of the circuit. In general, this corporate feed can be used with any type of microstrip array if the appropriate matching is done.

Parallel to the design of the corporate feed, the University of Massachusetts at Amherst developed the design of the antenna column with 69 elements, which means that the entire array has 4416 elements. Few antennas that operate at this frequency and with similar number of elements can be found in the Literature; generally, because the losses are difficult to handle and the feeding networks cannot be coplanar to the array. Using a combination of series and parallel feeds, this antenna demonstrated that an array of large numbers of elements and big size can be obtained if the feeding networks are handled properly.

During the summer of 2005 the corporate feed was integrated to the 64 columns to complete the microstrip array. The antenna has been built, but the measurement needs to be completed at another site as part of the future work because the size of the antenna exceeds the capabilities of the anechoic chambers available at both universities UMASS and UPRM.

As a part of the research into the transformation of the magnetron radar into a solid-state-radar, a surface mount transceiver was proposed. The principal limitations of this transceiver are its size and low efficiency; the need for a heat sink makes size reduction a more difficult subject even if the efficiency matter is solved. The results of these limitations, suggest that this surface-mount transceiver is not the most suitable solution for the deployment of a low cost solid state radar with electronic beam steering.

The author will continue his research in the area of phased arrays with microwave circuits. The purpose of this research is to design a transceiver using MMICs, which will overcome the limitations of space and efficiency of the surface mount transceiver; this will be done recurring to the work that has been developed in part and reported by [*Khandelwal, N., Jackson, R.,* 2005].

REFERENCES

Advance Design System Software, Available on http://www.agilent.com

Altshuler, E. E. and R. A. Marr, "A comparison of experimental and theoretical values of atmospheric absorption at the longer millimeter wavelengths," IEEE Trans. Antennas Propagation, vol. 36, no. 10, pp. 1471-1480, Oct. 1988.

Ansoft Designer, Available on http://www.ansoft.com

Balanis, C.A., "Antenna Theory: Analysis and Design", 2nd Ed. John Wiley & Sons Inc., 1996.

CASA Strategic Plan, 2003, Available from http://www.casa.umass.edu/

Dolph, C. L., "A Current Distribution for Broadside Arrays Which Optimizes the Relationship Between Beanwidth and Sidelobe Level", Proceedings of the I.R.E and Waves and Electrons, June 1946.

Douvile, R.J.P., James, D.S., "Experimental Study of Symmetric Microstrip Bends and Their Compensation", IEEE Microwave Theory and Techniques, Volume: 26 , Issue: 3 , Mar 1978.

Hall, P.S., Hall, C.M., "Coplanar corporate feed effects in microstrip patch array design", IEEE Proceedings-Microwaves, Antennas and Propagation, Volume: 135 , Issue: 3 , June 1988.

Horng,, T. S., Alexopoulos, N.G., "Corporate Feed Design for Microstrip Arrays", IEEE Transactions on Antennas and Propagation, Vol. 41 No 12, December 1993.

Huang, J., "Microstrip Antenna Developments at JPL", IEEE Antennas and Propagation Magazine, Vol 33, No 3, June 1991.

Huang, J., “Practical Design of Microstrip Arrays and Reflectarrays”, IEEE International Antennas and Propagation Symposium and USNC/CNC/URSI North American Radio Science Meeting, 2003.

Khandelwal, N., Jackson R., “ An X-band System-in-Package Active Antenna Module “, IEEE MTT-S International Microwave Symposium Digest Long Beach, CA, June 2005, Session WE4F-4.

Levyne, E., Malamud, G., Shtrikmanm, S., Treves, D., “A Study of Microstrip Array Antennas With The Feed Network”, IEEE Transactions on Antennas and Propagation, Vol. 37 No 4, April 1989.

PCAAD 3.0, Personal Computer Aided Antenna Design, Available on http://www.antennadesignassociates.com

Pozar, D. M., “Microwave Engineering”, 3rd Ed. John Wiley & Sons Inc., 2004.

Rogers Corporation, Available on http://www.rogers-corp.com/

Sawicki, A., Sachse, K., Jaworski, G., Kabacik, P., “Comparison of planar antenna feed networks with Wilkinson and coupled-line power divider”, 12th International Conference on Microwaves and Radar, Volume: 2 , 20-22 May 1998

Skolnik, M.I. “Introduction to Radar Systems”, 3rd Edition New York, NY. McGraw-Hill,2001.

Taconic Advanced Dielectric Division, Available on http://www.4taconic.com

Taylor, T. T., “One Parameter Family of Line Sources Producing Modified sin(πu)/πu Patterns”, Hughes Co. Tech. Mem.324, Culver City, Calif., Contract AF 19(604)-262-f-14, 1953.

Ulaby, F.T., Moore, R.K., Fung, A.K., “Microwave Remote Sensing: Active and Passive, Volume I: Fundamentals and Radiometry ”, Artech House, 1981.

Wang Chao-Fu, Feng Ling, Jian-Ming Jin, "A fast full-wave analysis of scattering and radiation from large finite arrays of microstrip antennas", IEEE Transactions on Antennas and Propagation, Vol. 46 No 10, October 1998.

Wang, J., Litva, J., "Design Study of A Low Sidelobe Microstrip Antenna Array and Feed Network", IEEE Antennas and Propagation Society International Symposium. Vol 2. June 1989.

APPENDIX A. DATA SHEETS

HMC232LP4
HMC347LP3
HMC487LP5
HMC441LP3
HMC516LC5
TRACK CIRCULATORS 2005